Kinetic data-driven approach to turbulence subgrid modeling

PHYSICAL REVIEW RESEARCH **7**, 013202 (2025)

Kinetic data-driven approach to turbulence subgrid modeling

G. Ortali,[1,2] A. Gabbana,[1,3] N. Demo,[2] G. Rozza,[2] and F. Toschi[1,3,4]

[1]*Department of Applied Physics and Science Education, Eindhoven University of Technology, 5600 MB Eindhoven, Netherlands*
[2]*SISSA (International School for Advanced Studies), I-34136 Trieste, Italy*
[3]*Eindhoven Artificial Intelligence Systems Institute, Eindhoven University of Technology, 5600 MB Eindhoven, Netherlands*
[4]*CNR-IAC, I-00185 Rome, Italy*

(Received 2 April 2024; accepted 11 February 2025; published 25 February 2025)

Numerical simulations of turbulent flows are well known to pose extreme computational challenges because of the huge number of dynamical degrees of freedom required to correctly describe the complex multiscale statistical correlations of the velocity. On the other hand, kinetic mesoscale approaches based on the Boltzmann equation, have the potential to describe a broad range of flows, stretching well beyond the special case of gases close to equilibrium, which results in the ordinary Navier-Stokes dynamics. Here, we demonstrate that, by properly tuning, a kinetic approach can statistically reproduce the quantitative dynamics of the larger scales in turbulence, thereby providing an alternative, computationally efficient and physically rooted approach toward subgrid scale (SGS) modeling in turbulence. More specifically, we show that by leveraging data from fully resolved direct numerical simulation (DNS), we can learn a collision operator for the discretized Boltzmann equation solver (the lattice Boltzmann method), which effectively implies a turbulence subgrid closure model. The mesoscopic nature of our formulation makes the learning problem fully local in both space and time, leading to reduced computational costs and enhanced generalization capabilities. We show that the model offers superior performance compared to traditional methods, such as the Smagorinsky model, being less dissipative and, therefore, able to more closely capture the intermittency of higher-order velocity correlations. This foundational study lays the basis for extending the proposed framework to different turbulent flow settings and—most importantly—to develop new classes of hybrid data-driven kinetic-based models capable of faithfully capturing the complex macroscopic dynamics of diverse physical systems such as emulsions, non-Newtonian fluid, and multiphase systems.

DOI: 10.1103/PhysRevResearch.7.013202

I. INTRODUCTION

Studying turbulent flows by means of fully resolved numerical simulations is known to pose outstanding computational challenges. The number of dynamical degrees of freedom, whose dynamics need to be accurately resolved, is typically huge as it rapidly grows as the 9/4 power of the Reynolds number (Re) [1–3]. Despite the ever-growing availability of computing resources, direct numerical simulations (DNS) of turbulent flows are still far out of reach for most real-world applications, strongly motivating a continuous effort toward the development of accurate and computationally cheaper reduced-order models. Alongside Reynolds-averaged Navier-Stokes (RANS) models [4], where the Navier-Stokes equations are averaged over time (separating the flow into mean and fluctuating components) large-eddy simulations (LES) [5] are among the most popular choices. In LES only a portion of the dynamical degrees of freedom, associated to the larger scales, is directly resolved, whereas the effect of the smaller scales on the large scales is parametrized by a subgrid-scale (SGS) model. In general, considering the filtered version of the macroscopic fields of interest, $\overline{\boldsymbol{u}}$ and $\overline{p}$ (respectively, velocity and pressure), one can write the Navier-Stokes equations filtered to describe only scales larger than ℓ,

$$\frac{\partial \overline{\boldsymbol{u}}}{\partial t} + \nabla \cdot (\overline{\boldsymbol{u}}\,\overline{\boldsymbol{u}} + \overline{\boldsymbol{T}}) = -\nabla \overline{p} + \nu \nabla^2 \overline{\boldsymbol{u}}. \tag{1}$$

In this filtered equation, we have assumed density $\rho = 1$, ν is the kinematic viscosity of the fluid and $\overline{\boldsymbol{T}} = \overline{\boldsymbol{u}\boldsymbol{u}} - \overline{\boldsymbol{u}}\,\overline{\boldsymbol{u}}$ is the Reynolds stress tensor, accounting for the SGS fluctuations, from which one can define a local subgrid energy flux [6]. The problem of defining an SGS closure consists of modeling the unknown term $\overline{\boldsymbol{T}}$ as a function of only the resolved velocity field $\overline{\boldsymbol{u}}$. Over the years, several approaches to SGS turbulence modeling have been developed, relying on specific assumptions to approximate the effects of the unresolved scales. The first SGS model was proposed by Smagorinsky [7] and, in view of its simplicity and stability, remains one of the commonly adopted approaches to estimate the action of smaller scales on the larger scales by means of an effective eddy viscosity, defined on the basis of the local derivatives of the resolved velocity field,

$$\overline{\boldsymbol{T}}^{\text{smag}} = 2\nu_t \overline{\boldsymbol{S}} - \overline{p}\boldsymbol{I}, \quad \nu_t = (C_s \Delta)^2 |\overline{\boldsymbol{S}}|, \tag{2}$$

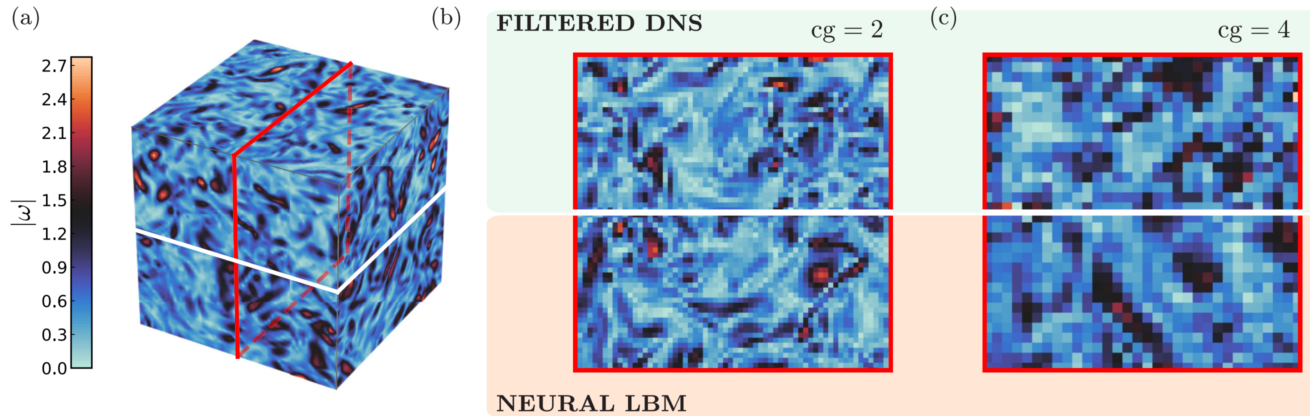

FIG. 1. Snapshots of the vorticity magnitude ($|\omega|$) from 3D simulations of HIT at Re $\approx$ 6000. In (a) the upper half of the domain is taken from filtered DNS data with cg = 2, while the lower half is obtained from a simulation using NBLM, trained and validated on the same flow conditions, albeit with different initial configurations. We show that at a qualitative level the structures generated by NLBM closely resemble those from filtered DNS. This is further highlighted in (b) and (c) where we show 2D slices of $|\omega|$ [cf. red box in (a)], respectively, at coarse-graining factor cg = 2 and cg = 4.

where $|\overline{\boldsymbol{S}}| = \sqrt{2\overline{S}_{ij}\overline{S}_{ij}}$, $\overline{S}_{ij} = 1/2(\partial_i \overline{u}_j + \partial_j \overline{u}_i)$ represents the magnitude of the filtered strain-rate, Δ is the filter width, and C_s is a nondimensional coefficient called the Smagorinsky constant. The Smagorinsky model has been shown to be a direct consequence of the refined Kolmogorov similarity hypothesis [8] and has been generalized to nonhomogeneous flows [9].

Other approaches have been introduced, including improvements to the Smagorinsky model that dynamically adjust the Smagorinsky constant C_s based on the flow field [10,11], and scale similarity models [12]. However, despite their widespread use, these models often face limitations in accurately representing the (statistical) properties of turbulent flows, particularly in scenarios with strong inhomogeneity and anisotropy.

Recent advances in machine learning have opened up new perspectives for employing artificial neural networks (ANN) [13] to enhance computational fluid dynamics solvers [14–17], and for the development of data-driven turbulence modeling [18–21]. Specifically to the LES context, several attempts have been reported in the literature [22–27] to establish SGS closure models from extensive datasets of fully resolved turbulent flows, leveraging the capability of ANN to handle high-dimensional and statistically complex data. In general, two main approaches have been adopted; the first, which can be regarded as the "black-box" approach, consists of making no assumption about the form of the SGS terms [28–31], while in the second the task of the ANN consists in tuning the free parameters of an already established SGS model [32–34].

In this paper we take a fresh look at the problem of establishing a SGS closure model with ANN, and introduce a data-driven kinetic-based approach to turbulence modeling. We employ physics-informed machine learning (PIML) to enhance the capabilities of the lattice Boltzmann method (LBM), and exploit the extra degrees of freedom provided by the mesoscopic description to learn a new collision operator, which effectively acts as SGS model. Our framework relies on the pathway connecting kinetic theory to hydrodynamics, offering the possibility to learn from data macroscopic equations that extend beyond the Navier-Stokes level. Specifically, we consider the problem of learning an SGS closure in the context of homogeneous isotropic turbulence (HIT) that reproduces the complex statistics of filtered DNS, including features such as intermittency and backscatter (an example is shown in Fig. 1). This represents an open problem in turbulence research and is considered here as a foundational step for the introduced framework, which could be extended to learn different physical problems. The proposed framework is inherently local owing to the locality of the collision operator [35], which contrasts with other ML approaches [19]. This drastically simplifies the training process and enhances the interpretability of the model. Remarkably, and at variance with respect to other fully local SGS models, our formalism shows the potential for capturing the inverse transfer of energy from small to large scales, without causing numerical instabilities.

II. METHODS

The lattice Boltzmann method (LBM) [36–38] has emerged in the past decades as a popular solver for computational fluid dynamics. At variance with methods that explicitly discretize the Navies-Stokes equations, LBM operates at the mesoscopic level, providing the description of a fluid system in terms of a (small) set of particle distribution functions (populations) whose dynamic is governed by the discrete Boltzmann equation

$$f_i(\boldsymbol{x} + \boldsymbol{c}_i \Delta t, t + \Delta t) = f_i(\boldsymbol{x}, t) + \Omega_i(\boldsymbol{x}, t), \quad (3)$$

where at each grid node $\boldsymbol{x}$, lattice populations $f_i(\boldsymbol{x}, t)$ represent the probability distribution function of particles at position $\boldsymbol{x}$ and time t moving with discrete velocity $\boldsymbol{c}_i$, $i = 1, \dots, Q$. The uninitiated reader can find a more detailed introduction to the lattice Boltzmann method within the Supplemental Material (SM) [39]. A popular choice for the collision operator Ω is the single-time relaxation BGK model [40],

$$\Omega_i(\boldsymbol{x}, t) = -\frac{\Delta t}{\tau}\big(f_i(\boldsymbol{x}, t) - f_i^{\text{eq}}(\boldsymbol{x}, t)\big), \quad (4)$$

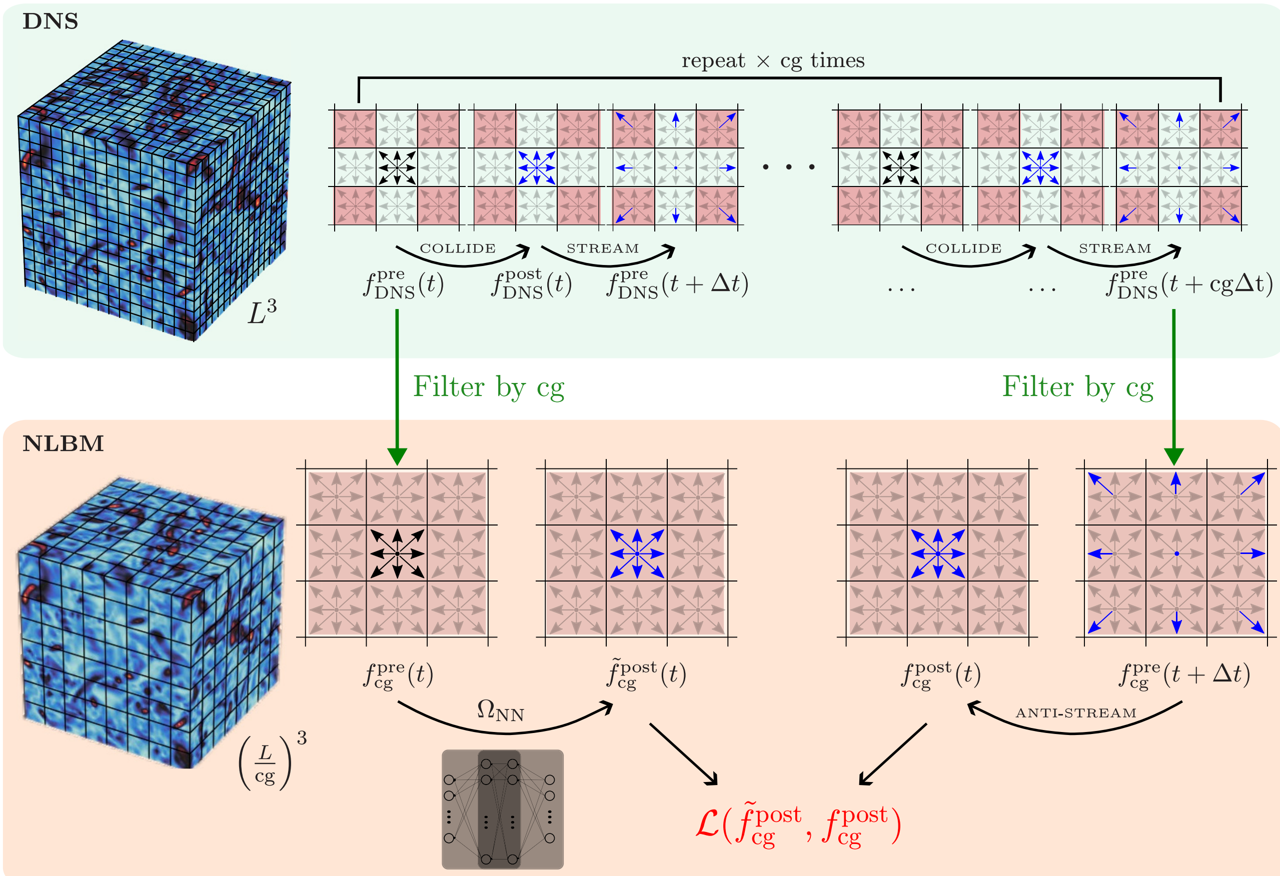

FIG. 2. Schematic representation of the training process for the turbulence SGS model. The upper panel corresponds to the DNS simulation on a L^3 grid, while in lower panel the neural LBM (NLBM) operates on a $(L/\mathrm{cg})^3$ grid, with coarse-graining factor cg via subsampling. The mapping between DNS into coarse-grained data is given by the application of a filter: the precollision state at a generic time step t at the coarse-grained level $[f_{\mathrm{cg}}^{\mathrm{pre}}(t)]$ is obtained by filtering the DNS precollision state $[f_{\mathrm{DNS}}^{pre}(t)]$ (dependence on space has been omitted for conciseness). Similarly, the postcollision data at the coarse-grained level $[f_{\mathrm{cg}}^{\mathrm{post}}(t)]$ is obtained by first filtering the postcollision DNS state at time step $t+\mathrm{cg}\Delta t$, and then by applying the inverse of the streaming operator. Following this procedure it is possible to create a dataset of arbitrary size for training an ANN to which we assign the task of minimizing the mismatch between $\tilde{f}_{\mathrm{cg}}^{\mathrm{post}}(t)=\Omega_{\mathrm{NN}}(f_{\mathrm{cg}}^{\mathrm{pre}}(t))$ and $f_{\mathrm{cg}}^{\mathrm{post}}(t)$ under a given error metric $\mathcal{L}$.

which models collisions as a relaxation towards an equilibrium distribution, with τ the relaxation rate. The macroscopic variables of interest can be obtained as the lower-order moments of the lattice populations. Moreover, it can be shown via an asymptotic analysis that Eq. (3) yields a second-order approximation of the Navier-Stokes equations [38].

It is an expedient for the description of our method to split the time evolution of Eq. (3) into two steps, following the *stream* and *collide* paradigm:

$$f_i^{\mathrm{post}}(\boldsymbol{x},t)=f_i^{\mathrm{pre}}(\boldsymbol{x},t)+\Omega_i(\boldsymbol{x},t), \tag{5}$$

$$f_i^{\mathrm{pre}}(\boldsymbol{x},t+\Delta t)=f_i^{\mathrm{post}}(\boldsymbol{x}-\boldsymbol{c}_i\Delta t,t), \tag{6}$$

where here and in what follows we will denote with f_i^{pre} (f_i^{post}) the pre(post)collision populations.

Following the framework introduced in Ref. [41], we replace the collision operator with a ANN, effectively defining a generalized collision operator

$$\tilde{f}_i^{\mathrm{post}}(\boldsymbol{x},t)=f_i^{\mathrm{pre}}(\boldsymbol{x},t)+\Omega^{\mathrm{NN}}\big(f_i^{\mathrm{pre}}(\boldsymbol{x},t)\big). \tag{7}$$

The resulting algorithm, to which we refer as neural lattice Boltzmann method (NLBM), employs a physics-constrained ANN to establish a data-driven SGS model. Our approach leverages on two key ingredients of the LBM algorithm:

(1) The LBM mesoscopic representation makes use of a larger number of degrees of freedom (i.e., the number of discrete lattice populations) than the macroscopic observable of interest. This observation opens up the possibility of using ANN to encode extra information in the model.

(2) The nonlinear terms encountered at the NS level of description [cf. Eq. (1)] are fully embedded in the LBM via the collision operator and thus purely local (in LBM "nonlinearity is local, nonlocality is linear" [37]). This observation drastically reduces the cost of training ANN, since it offers the possibility to restrict the input and output of the network to local quantities without explicit evaluation of gradients of macroscopic fields.

We summarize here the main steps required to train the ANN, as sketched in Fig. 2, leaving full technical details to the SM [39]. We consider simulations of homogeneous isotropic turbulence (HIT), fully resolved on a L^3 domain using the standard LBM formulation [Eq. (3)] with BGK collision operator [Eq. (4)]. We regard this as the target ground truth DNS data (upper panel in Fig. 2). Next, we define a coarse-graining factor cg, and define a filter, which projects, at a given time step t, data from the DNS grid to a coarse-grained grid of size $(L/\mathrm{cg})^3$, where the SGS model will operate (lower panel in Fig. 2). In order to define an arbitrarily large training dataset consisting of pre and postcollision data at the coarse-grained level, respectively $f_{\mathrm{cg}}^{\mathrm{pre}}(t)$ and $f_{\mathrm{cg}}^{\mathrm{post}}(t)$, we take the following steps: We start from the precollision populations at the DNS level, $f_{\mathrm{DNS}}^{\mathrm{pre}}(t)$, and immediately apply the filter in order to obtain $f_{\mathrm{cg}}^{\mathrm{pre}}(t)$. Next, we advance the DNS simulation for cgΔt time steps, yielding the precollision (and post-streaming) populations $f_{\mathrm{DNS}}^{\mathrm{pre}}(t + \mathrm{cg}\Delta \mathrm{t})$. Since Δt steps at the coarse-grained level correspond to cgΔt steps at the DNS level, by filtering $f_{\mathrm{DNS}}^{\mathrm{pre}}(t + \mathrm{cg}\Delta \mathrm{t})$ we obtain $f_{\mathrm{cg}}^{\mathrm{pre}}(t + \Delta t)$. Finally, we obtain $f_{\mathrm{cg}}^{\mathrm{post}}(t)$ by reversing the streaming operation, i.e., we anti-stream populations on the coarse grid with respect to the corresponding velocity component $-\boldsymbol{c}_i$ taken from the coarse-grid velocity stencil.

At this stage, we can train a ANN which, under a given error metric $\mathcal{L}$, minimizes the mismatch between $f_{\mathrm{cg}}^{\mathrm{post}}(t)$ and the prediction of the network taking $f_{\mathrm{cg}}^{\mathrm{pre}}(t)$ as input,

$$\mathcal{L}\big(\Omega^{\mathrm{NN}}\big(f_{\mathrm{cg}}^{\mathrm{pre}}(t)\big), f_{\mathrm{cg}}^{\mathrm{post}}(t)\big). \tag{8}$$

We have observed that the two main ingredients allowing for training models, which deliver accurate and stable results throughout an entire simulation are (i) imposing hard constraints on the preservation of mass and momentum [41] and (ii) using *unrolled training* [42] to compute the loss over consecutive time steps. Full details on the ANN architecture, the training process, and the complete form of the loss function are provided within the SM [39].

III. NUMERICAL RESULTS

We consider numerical simulations of HIT, with for reference a DNS on a $L = 128^3$ grid at Reynolds number Re $\approx$ 6000 (corresponding to a Taylor microscale Reynolds number $\mathrm{Re}_\lambda \approx 77$). The parameters are selected in such a way that the plain LBM algorithm would encounter numerical instabilities when working on coarse-grained grids with cg = {2, 4}. Fig. 1 qualitatively summarizes our findings. Starting from the same initial configuration, we present 3D and 2D representations of the absolute value of the vorticity $|\boldsymbol{\omega}| = |\nabla \times \boldsymbol{u}|$ at a late stage of the simulation, comparing results from the filtered DNS with NLBM. Our model provides stable simulations, with flow patterns virtually indistinguishable from those of the filtered DNS.

On a more quantitative level, we now turn to the evaluation of the statistical properties of the turbulent flows produced by NLBM simulations. For comparison, we include LBM simulations equipped with the Smagorinsky SGS model [Eq. (2)] as a standard reference point. The Smagorinsky model is chosen in this context for its well-known and widely understood properties within the context of HIT. In Fig. 3 we present the kinetic energy spectrum $E(k)$. We observe that NLBM compares well with the results produced by Smagorinsky, with slightly superior results at cg = 4, where we can observe a spectrum that is less dissipative than the Smagorinsky one and

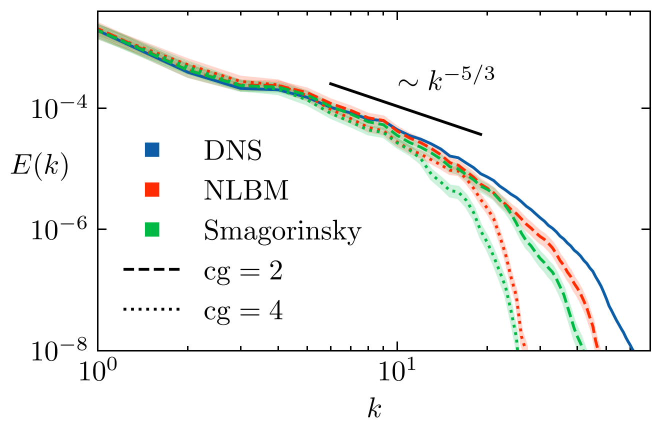

FIG. 3. Energy spectrum for simulations of HIT at Re $\approx$ 6000. The results from DNS (blue curve) are compared with NLBM (red) and Smagorinsky (green). For the two SGS models, we report the average spectrum from 80 simulations starting from different initial conditions. The shaded curves corresponds to one standard deviation from the average value.

closer to the scaling of DNS data. Next, we study the scaling behavior of high-order Eulerian structure function, which for a generic order p can be computed from numerical data as

$$S^p(l) = \langle [(\boldsymbol{u}(\boldsymbol{x} + \boldsymbol{l}) - \boldsymbol{u}(\boldsymbol{x})) \cdot \hat{\boldsymbol{l}}]^p \rangle. \tag{9}$$

We use the extended self-similarity (ESS) [43] to determine the scaling exponents ξ_p. In Fig. 4, we plot the structure functions of order p, ranging between $p = 1$ to $p = 6$, versus $S^3(l)$, comparing data from filtered DNS with cg = 4, and data from simulations using NLBM and the Smagorinsky

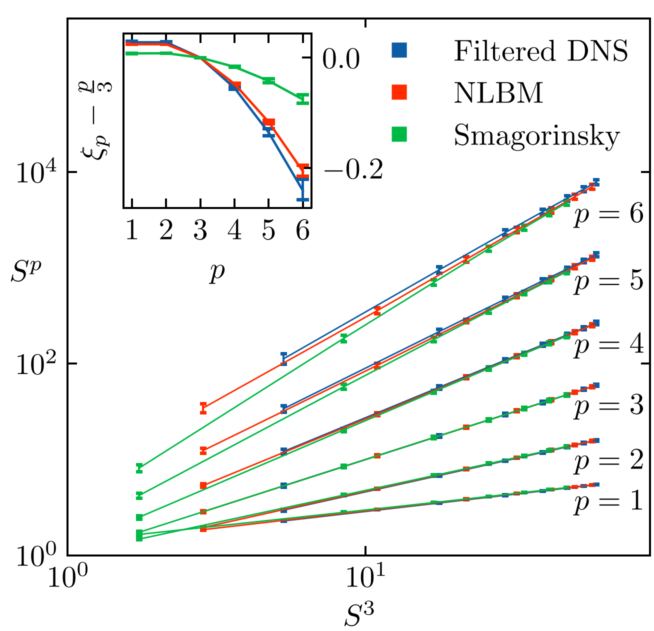

FIG. 4. Structure functions [cf. Eq. (9)] of order p, ranging between $p = 1$ to $p = 6$, vs S^3, with in blue data from filtered DNS with cg = 4, in red data from simulations using NLBM, and in green data from simulations using the Smagorinsky model. The inset shows the deviation for the scaling exponents ξ_p from the K41 scaling $\frac{p}{3}$.

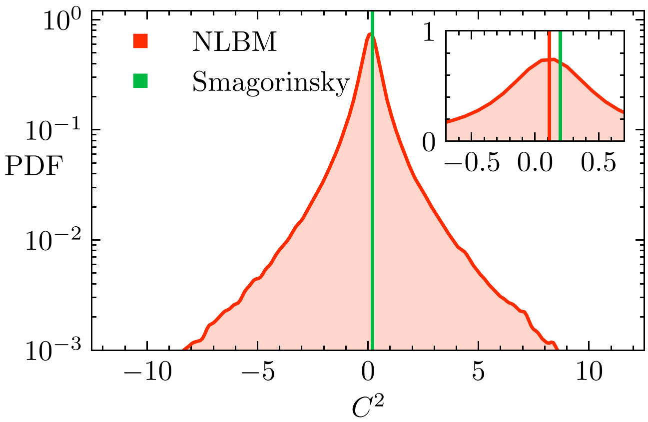

FIG. 5. Probability distribution function (PDF) of the fitted value of the Smagorinsky constant C^2 from NLBM data. The inset highlights that the average value $\langle C^2_{\text{NLBM}} \rangle \approx 0.11$ is about a factor two smaller than the one used in simulations with the Smagorinsky SGS model ($C^2 = 0.2$). The presence of a tail with negative values highlights the fact that in NLBM it is possible to capture the inverse transfer of energy from small to large scales.

model. In the inset of Fig. 4, we report the deviation of ξ_p from the K41 scaling $p/3$. The results highlight that, due to its lower dissipation at small scales, NLBM provides anomalous scaling within error bars from filtered DNS. On the other hand, the discrepancies observed in the Smagorinsky model stem from the fact that under these parameters the inertial range is shrunk (see the SM [39] for a more detailed analysis).

A major advantage of our kinetic-based approach lies in the possibility of physically interpretating the action of the ANN by projecting the lattice populations to the velocity moment space (see the SM [39]). We have observed that NLBM extends the single-relaxation BGK collision operator, from where DNS data was generated, to a multirelaxation collision operator [44,45]. The model introduces a nonlinear relation between precollision and postcollision values of the moments related to the bulk viscosity, something, which is often used to increase the stability of numerical simulations. The model preserves a linear dependence for the precollision and postcollision values of the moments related to the kinetic viscosity. This allows us to fit the effective viscosity from the numerical data, which can be used to establish a direct comparison with the Smagorinsky model [Eq. (2)]. In Fig. 5 we compare the probability distribution function (PDF) of the value of the Smagorinsky constant C^2 fitted from NLBM data (cg = 4). The average value of the Smagorinsky constant for NLBM ($\langle C^2_{\text{NLBM}} \rangle \approx 0.11$) is about a factor of two smaller than the one used in simulations with the Smagorinsky SGS model ($C^2 = 0.2$). Remarkably, in Fig. 5 we observe a tail extending into negative values, suggesting that our model occasionally displays an inverse transfer of energy from small to large scales—a feature completely lacking to the Smagorinsky model, which is, by its nature, fully dissipative.

IV. CONCLUSIONS

Summarizing, we have introduced a kinetic-based approach to SGS modeling, combining LBM with physics-informed ANN. Our model allows for stable simulations on coarse domains, offering the possibility of reducing the computational costs of DNS, while preserving the statistical properties of turbulent flows under HIT settings. The model compares well with Smagorinsky, and our results highlight a better agreement with DNS in terms of energy spectra and estimation of the anomalous scaling exponents. Moreover, we have shown that the model in principle supports the possibility of describing the inverse transfer of energy from small to large scales, which we regard as promising particularly with a view to future applications to more involved numerical setups. To conclude, this paper opens up the possibility of exploiting the extra degrees of freedom in the mesoscopic representation in the LBM to develop novel SGS models. In future works, we plan to extend our analysis to flows subject to anisotropy as well as wall-bounded flows. A further intriguing question concerns the application of this framework beyond SGS. Work exploring our kinetic data-driven approach in other contexts is currently underway.

ACKNOWLEDGMENTS

We wish to thank Roberto Benzi for useful discussions. This work was partially funded by the Dutch Research Council (NWO) through the UNRAVEL project (with Project No. OCENW.GROOT.2019.044).

[1] U. Frisch, *Turbulence: The Legacy of A.N. Kolmogorov* (Cambridge University Press, Cambridge, 1995).
[2] S. B. Pope, *Turbulent Flows* (Cambridge University Press, Cambridge, 2000).
[3] R. Benzi and F. Toschi, Lectures on turbulence, Phys. Rep. **1021**, 1 (2023).
[4] G. Alfonsi, Reynolds-averaged Navier–Stokes equations for turbulence modeling, Appl. Mech. Rev. **62**, 040802 (2009).
[5] Y. Zhiyin, Large-eddy simulation: Past, present and the future, Chin. J. Aeronaut. **28**, 11 (2015).
[6] V. Borue and S. A. Orszag, Local energy flux and subgrid-scale statistics in three-dimensional turbulence, J. Fluid Mech. **366**, 1 (1998).
[7] J. Smagorinsky, General circulation experiments with the primitive equations: I. The basic experiment, Mon. Weather Rev. **91**, 99 (1963).
[8] F. Toschi, E. Lévêque, and G. Ruiz-Chavarria, Shear effects in nonhomogeneous turbulence, Phys. Rev. Lett. **85**, 1436 (2000).
[9] E. Lévêque, F. Toschi, L. Shao, and J-P. Bertoglio, Shear-improved Smagorinsky model for large-eddy simulation of wall-bounded turbulent flows, J. Fluid Mech. **570**, 491 (2007).
[10] M. Germano, U. Piomelli, P. Moin, and W. H. Cabot, A dynamic subgrid–scale eddy viscosity model, Phys. Fluids **3**, 1760 (1991).
[11] S. Ghosal, T. S. Lund, P. Moin, and K. Akselvoll, A dynamic localization model for large-eddy simulation of turbulent flows, J. Fluid Mech. **286**, 229 (1995).

[12] C. Meneveau and J. Katz, Scale-invariance and turbulence models for large-eddy simulation, Annu. Rev. Fluid Mech. **32**, 1 (2000).
[13] I. Goodfellow, Y. Bengio, and A. Courville, *Deep Learning* (MIT Press, Cambridge, MA, 2016).
[14] D. Kochkov, J. A. Smith, A. Alieva, Q. Wang, M. P. Brenner, and S. Hoyer, Machine learning–accelerated computational fluid dynamics, Proc. Natl. Acad. Sci. USA **118**, e2101784118 (2021).
[15] R. Vinuesa and S. L. Brunton, Enhancing computational fluid dynamics with machine learning, Nat. Comput. Sci. **2**, 358 (2022).
[16] M. Lino, S. Fotiadis, A. A. Bharath, and C. D. Cantwell, Current and emerging deep-learning methods for the simulation of fluid dynamics, Proc. R. Soc. A: Math., Phys. Engn. Sci. **479**, 20230058 (2023).
[17] S. L. Brunton, B. R. Noack, and P. Koumoutsakos, Machine learning for fluid mechanics, Annu. Rev. Fluid Mech. **52**, 477 (2020).
[18] G. Novati, H. L. de Laroussilhe, and P. Koumoutsakos, Automating turbulence modelling by multi-agent reinforcement learning, Nat. Mach. Intell. **3**, 87 (2021).
[19] J. Ling, A. Kurzawski, and J. Templeton, Reynolds averaged turbulence modelling using deep neural networks with embedded invariance, J. Fluid Mech. **807**, 155 (2016).
[20] K. Duraisamy, G. Iaccarino, and H. Xiao, Turbulence modeling in the age of data, Annu. Rev. Fluid Mech. **51**, 357 (2019).
[21] R. Wang, K. Kashinath, M. Mustafa, A. Albert, and R. Yu, Towards physics-informed deep learning for turbulent flow prediction, in *Proceedings of the 26th ACM SIGKDD International Conference on Knowledge Discovery & Data Mining, KDD '20* (ACM, New York, 2020), pp. 1457–1466.
[22] Z. Wang, K. Luo, D. Li, J. Tan, and J. Fan, Investigations of data-driven closure for subgrid-scale stress in large-eddy simulation, Phys. Fluids **30**, 125101 (2018).
[23] R. Maulik, O. San, A. Rasheed, and P. Vedula, Subgrid modelling for two-dimensional turbulence using neural networks, J. Fluid Mech. **858**, 122 (2019).
[24] C. Xie, J. Wang, and W. E, Modeling subgrid-scale forces by spatial artificial neural networks in large eddy simulation of turbulence, Phys. Rev. Fluids **5**, 054606 (2020).
[25] J. Park and H. Choi, Toward neural-network-based large eddy simulation: Application to turbulent channel flow, J. Fluid Mech. **914**, A16 (2021).
[26] H. Frezat, G. Balarac, J. Le Sommer, R. Fablet, and R. Lguensat, Physical invariance in neural networks for subgrid-scale scalar flux modeling, Phys. Rev. Fluids **6**, 024607 (2021).
[27] Y. Tian, M. Woodward, M. Stepanov, C. Fryer, C. Hyett, D. Livescu, and M. Chertkov, Lagrangian large eddy simulations via physics-informed machine learning, Proc. Natl. Acad. Sci. USA **120**, e2213638120 (2023).
[28] A. Beck, D. Flad, and C.-D. Munz, Deep neural networks for data-driven LES closure models, J. Comput. Phys. **398**, 108910 (2019).
[29] Z. Zhou, G. He, S. Wang, and G. Jin, Subgrid-scale model for large-eddy simulation of isotropic turbulent flows using an artificial neural network, Comput. Fluids **195**, 104319 (2019).
[30] C. Xie, J. Wang, K. Li, and C. Ma, Artificial neural network approach to large-eddy simulation of compressible isotropic turbulence, Phys. Rev. E **99**, 053113 (2019).
[31] M. Kurz, P. Offenhäuser, and A. Beck, Deep reinforcement learning for turbulence modeling in large eddy simulations, Int. J. Heat Fluid Flow **99**, 109094 (2023).
[32] F. Sarghini, G. de Felice, and S. Santini, Neural networks based subgrid scale modeling in large eddy simulations, Comput. Fluids **32**, 97 (2003).
[33] C. Xie, J. Wang, H. Li, M. Wan, and S. Chen, Artificial neural network mixed model for large eddy simulation of compressible isotropic turbulence, Phys. Fluids **31**, 085112 (2019).
[34] Y. Wang, Z. Yuan, C. Xie, and J. Wang, Artificial neural network-based spatial gradient models for large-eddy simulation of turbulence, AIP Adv. **11**, 055216 (2021).
[35] H. Chen, S. Kandasamy, S. Orszag, R. Shock, S. Succi, and V. Yakhot, Extended Boltzmann kinetic equation for turbulent flows, Science **301**, 633 (2003).
[36] R. Benzi, S. Succi, and M. Vergassola, The lattice Boltzmann equation: Theory and applications, Phys. Rep. **222**, 145 (1992).
[37] S. Succi, *The Lattice Boltzmann Equation: For Complex States of Flowing Matter* (Oxford University Press, Oxford, 2018).
[38] T. Krüger, H. Kusumaatmaja, A. Kuzmin, O. Shardt, G. Silva, and E. M. Viggen, *The Lattice Boltzmann Method* (Springer, New York, 2017).
[39] See Supplemental Material at http://link.aps.org/supplemental/10.1103/PhysRevResearch.7.013202 for more details on the numerical method and neural network architecture.
[40] P. L. Bhatnagar, E. P. Gross, and M. Krook, A model for collision processes in gases. Amplitude processes in charged and neutral one-component systems, Phys. Rev. **94**, 511 (1954).
[41] A. Corbetta, A. Gabbana, V. Gyrya, D. Livescu, J. Prins, and F. Toschi, Toward learning lattice Boltzmann collision operators, Eur. Phys. J. E **46**, 10 (2023).
[42] J. Brandstetter, D. Worrall, and M. Welling, Message passing neural PDE solvers, arXiv:2202.03376.
[43] R. Benzi, S. Ciliberto, R. Tripiccione, C. Baudet, F. Massaioli, and S. Succi, Extended self-similarity in turbulent flows, Phys. Rev. E **48**, R29 (1993).
[44] P. Lallemand and L.-S. Luo, Theory of the lattice boltzmann method: Dispersion, dissipation, isotropy, galilean invariance, and stability, Phys. Rev. E **61**, 6546 (2000).
[45] D. D'Humières, I. Ginzburg, M. Krafczyk, P. Lallemand, and L.-S. Luo, Multiple-relaxation-time lattice Boltzmann models in three dimensions, Philos. Trans. R. Soc. London **360**, 437 (2002).